Chapter 5
Cytarabine loaded PLGA based nanoparticles

CHAPTER 5
FORMULATION DEVELOPMENT AND EVALUATION OF CYTARABINE LOADED PLGA AND PLGA-MPEG NANOPARTICLES

5.1 Materials

Cytarabine was obtained as a gift sample from Biocon, Bangalore, Poly (DL lactide-co-glycolide) PLGA 50:50 (inherent viscosity 0.22 dl/g) was obtained as a gift sample from Boehringer Ingelheim Limited, Germany, Pluronic F-68 (BASF) was obtained as a gift sample from Alembic Ltd, Vadodara. Chloroform, Methanol, Acetone, Potassium dihydrogen phosphate, Disodium hydrogen phosphate, Hydrochloric acid and Sodium hydroxide were obtained form SD fine Chemicals, Mumbai, Synthetic cellulose membrane (MWCO12,000) was procured from Himedia Labs, Mumbai.

5.2 Formulation development of Cytarabine loaded PLGA and PLGA-mPEG Nanoparticles

Modified nanoprecipitation method was used for the preparation of nanoparticles (Peltonen et al., 2004). Hydrophilic drug (5mg of CYT) was dissolved in an aqueous phase consisting of a solvent (0.3 ml of distilled water) and a co-solvent (0.6 ml of methanol). Polymer (25 mg of PLGA) was dissolved in an organic phase consisting of a non-solvent (4ml of chloroform). The organic phase was then added drop wise to aqueous phase under stirring. Finally, the above mixture was added drop wise to 10 ml of distilled water containing 0.5% w/v of Pluronic F-68. Organic solvent was removed by stirring over night. Nanoparticles were then recovered from the nanodispersion by centrifugation (Sigma centrifuge) for 30 min at 25000 rpm, washed two times with distilled water to remove unentrapped drug. The dispersion was finally lyophilized (Heto Dry Winner, Denmark) for 24 hrs to yield freeze dried nanoparticles. Samples were frozen at −70 °C and placed immediately in the freeze-drying chamber. Different concentrations of sucrose in 10, 20, 50, 75 and 100% w/w of the total solid content were used as cryoprotectant.

The method was first optimized for choice of co-solvent based on MPS. Three batches in triplicate were taken, first without a co-solvent, second with acetone and third with

methanol. Then a 3^2 factorial design was used for the optimization of volume of co-solvent and non solvent based on MPS of the nanoparticles obtained. Contour plots and response surface curves were plotted to give a diagrammatic representation of the values of the response. A 3^2 factorial design was also used for the optimization drug: polymer ratio and stirring time based on MPS and % entrapment efficiency of the nanoparticles. The flow chart of the method showing different steps in the formation of nanoparticles is shown in Fig.5.1.

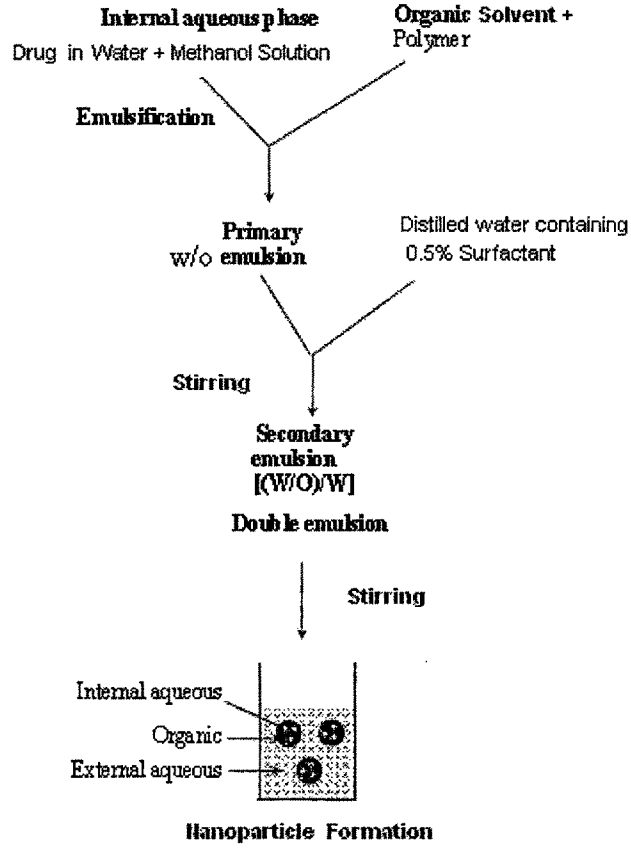

Fig. 5.1: Flow diagram for formulation of NP

Similarly, cytarabine loaded PLGA-mPEG NPs were prepared by using PLGA-MPEG (synthesis and characterization of the block copolymer is explained in section 4.7 and 4.9) instead of PLGA. A 3^2 factorial design was used for the optimization of drug:polymer ratio and volume of non-solvent based on MPS and % entrapment efficiency of the nanoparticles.

5.3 Evaluation of Nanoparticles

The prepared Nanoparticles were evaluated for mean particle size, entrapment efficiency, surface charge, SEM, DSC, XRD, in vitro drug release study, drug release kinetics and stability studies. The methods used were same as those described under section 4.4 except for entrapment efficiency and in vitro drug release study.

Entrapment efficiency

The entrapment efficiency was determined by extracting and quantifying the encapsulated drug using UV- spectroscopy. 100mg of NPs were added to 10 ml of 1:1 mixture of chloroform and methanol. This dispersion was subjected to shaking at room temperature to ensure complete dissolution of the particles, the resulting solution was evaporated to dryness, and the dried residue was reconstituted with 5 ml of phosphate buffer saline. The reconstituted dispersion was centrifuged at 10000 rpm for 15 min. In this extraction procedure, the drug was solubilised in PBS and the polymer which was not soluble remained in the pellet. The supernatant was analyzed for drug using UV-spectroscopy at λ_{max} 271 nm using calibration curve of cytarabine in PBS as explained in section 3.3.1. The % entrapment efficiency (EE) was calculated using the following formula-

% EE = (Amount of drug in the NPs/drug added in the formulation) * 100

Redispersibility of lyophilized nanoparticles

We used two methods for redispersing the lyophilized NP, manual shaking and sonication (Freitas and Muller, 1998). First method used was manually shaking a weighed quantity of lyophilized NP (100mg) in a test tube containing 5ml of phosphate buffer saline pH 7.4. After gentle shaking for two minutes the nanosuspension was subjected to particle size measurement using Malvern zetasizer. Presence of particles of more than 1micron were said to non dispersible. In the second method, 100mg of the lyophilized NP in a test tube containing 5ml of phosphate buffer saline pH 7.4 was subjected to sonication for 2 minutes using a bath sonicator and redispersibility was checked as explained above.

In -vitro drug release study

The dialysis bag diffusion technique was used to evaluate the in vitro drug release (Levy and Benita, 1990). The NP corresponding to 10 mg of cytarabine was placed in a dialysis bag with a molecular weight cut-off (MWCO) of 12,000–14,000 D (Sigma, USA) which was tied and placed into 200 ml of phosphate buffer saline (PBS) maintained at 37°C with continuous magnetic stirring in a beaker. At predetermined time intervals, aliquots were withdrawn from the acceptor compartment and replaced by the same volume of PBS. The drug content of the samples was determined by UV spectrophotometer at 271 nm. The tests were carried out three times and cumulative percentage drug release was calculated. The data was statistically analyzed using the Sigmastat software (Sigma Stat, USA).

5.4 Results and Discussions

In the nanoprecipitation method, an organic solution of the polymer is emulsified in an aqueous solution (with or without a surfactant). Then the organic solvent is removed by stirring (with or without vacuum) and this process allows nanoparticle formation. This method has drawback if the drug to be encapsulated is hydrophilic, because the drug may leak out in the aqueous solution. Hence we modified the method and as suggested by Peltonen et al. (2004), we used a double emulsion technique in which the aqueous solution of the hydrophilic compound was first emulsified in an organic solution of the polymer and then this primary emulsion was poured into a large volume of water with surfactant.

5.4.1 Choice of co-solvent

For the optimization of choice of co-solvent, the different formulation conditions and MPS obtained are shown in Table 5.1. With acetone, the particle size achieved was higher compared with methanol because of the tendency of drug substance to precipitate in the presence of acetone. Based on the least MPS (138nm) obtained for batch No. CPNP3, methanol was chosen as the co-solvent.

Table 5.1
Effect of co-solvent on mean particle size of Cyt-PLGA NP

Batch No.	Aqueous Phase (1 ml)		Organic phase (4ml)		MPS (nm) ± SD
	Drug (mg)	Volume of Co-solvent	Polymer PLGA (mg)	Volume of chloroform (ml)	
CPNP1	5	No co-solvent	25	4	250 ±12.0
CPNP2	5	Acetone, 0.3 ml	25	4	195±6.2
CPNP3	5	Methanol 0.3 ml	25	4	138±7.8

5.4.2 Optimization of volume of co-solvent and non solvent by factorial design for formulation of Cytarabine loaded PLGA NP

Nine batches were prepared as per 3^2 factorial design to study the effect of two independent variables, volume of the co-solvent (X1) and volume of non solvent (X2) on the response, mean particle size (Y1) of the Cyt-PLGA Nanoparticles. Table 5.2 displays the values of Factors, their levels and transformed values and values of the response MPS as per 3^2 factorial design.

Table 5.2
Formulation of Cyt-PLGA NP for optimization of volume of co-solvent and non solvent. Batches taken as per 3^2factorial design: Factors, their levels and transformed Values and Response: MPS

	Real value		Transformed values					Response
Batch No.	Volume of the co-solvent (ml)	Volume of the Non solvent (ml)	X1	X2	$X1^2$	$X2^2$	X1X2	MPS (nm) ± SD*
CPNP4	0.3	2	-1	-1	1	1	1	147 ±7.1
CPNP5	0.3	4	-1	0	1	0	0	137 ±2.3
CPNP6	0.3	8	-1	1	1	1	-1	142 ±6.2
CPNP7	0.6	2	0	-1	0	1	0	137 ±7.6
CPNP8	**0.6**	**4**	**0**	**0**	**0**	**0**	**0**	**127 ±3.1**
CPNP9	0.6	8	0	1	0	1	0	134 ±5.2
CPNP10	0.9	2	1	-1	1	1	-1	141 ±3.4
CPNP11	0.9	4	1	0	1	0	0	137 ±2.5
CPNP12	0.9	8	1	1	1	1	1	148 ±5.6

*Standard Deviation (n=3)

Response-Mean Particle Size

The equations for full model for Y1 (MPS) is given by equation 5.1

$$Y1\ (MPS) = 127.44+0.0X1-0.16X2+9.33X1^2+7.83X2^2+3.0X1X2 \qquad (5.1)$$

The mean particle size of NP ranged from 127±3.1 to 148±5.6 nm. The lowest MPS was observed in middle level of X1 (0.3 ml) and middle level of X2 (2.0 ml) in batch CPNP8.

Table 5.3 shows model coefficients estimated by multiple linear regression for MPS. The regression coefficients having P value < 0.05 are highly significant. The terms having coefficients with P value > 0.05 are least contributing in the prediction of mean particle size and hence the factor X1X2 having P value > 0.05 was removed from the full model to give the reduced model equation.

The equation 5.2 explains the reduced model for Y1 (MPS).

$$Y1\ (MPS) = 127.44+0.0X1-0.16X2+9.33X1^2+7.83X2^2+3.0X1X2 \qquad (5.2)$$

Table 5.3
Model Coefficients Estimated By Multiple Linear Regression For MPS

	Full model			Reduced model		
Factor	Coefficient value	Computed t-value	P-value	Coefficient value	Computed t-value	P-value
Intercept	127.444	123.207	1.18E-06	127.444	156.814	2E-10
X1	0	0	1			
X2	-0.166	-0.294	0.787			
$X1^2$	9.333	9.511	0.002	9.333	12.105	6.79E-05
$X2^2$	7.833	7.982	0.004	7.833	10.159	0.000158
X1X2	3	4.323	0.022	3	5.502	0.002709

Analysis of Variance (ANOVA) of Full and Reduced Model for MPS is shown in Table 5.4. Model F value is assessed by the F statistic, which estimates the percentage of the variability in the outcome explained by the model (Hocking RR. 1976). Full model F value (34.5923) was more than the tabulated F value (F_{tab} = 9.01), implying that the model was significant. Model F value of the reduced model is 93.34891and the F_{tab} value is 5.41, showing that the model is significant.

Table 5.4
Analysis of Variance (ANOVA) of Full and Reduced Model for MPS

	Full model		Reduced model	
	Regression	Error	Regression	Error
DF	5	3	3	5
SS	333.111	5.7777	332.944	5.9444
MS	66.622	1.9259	110.981	1.1888
F	34.592		93.348	
Significance f	0.00744		8.25E-05	
R^2	0.9829		0.9824	
Adj R^2	0.9545		0.9719	

The R^2 value is a measure of total variability explained by the model. The R^2 value of 0.98295 for the full model indicates that the model is significant. That means the model can explain 98.29% of varibility around the mean. R^2 of the reduced model is 0.982459, which is also high but slightly lower than the full model. The number of factors in the full model are more than the reduced model, therefore the R^2value increases (Montegomery, 2004). This explains the higher R^2 value of the full model than the reduced model. In such cases the term R^2 adjusted has to be checked. It is called adjusted as the value has been adjusted for the size of the model. The R^2 adjusted decreases when non significant terms are added to the equation. Removal of non significant terms improves the value of

R^2 adjusted. In our present model the value of R^2 adjusted in the reduced model is 0.982459, which is greater than the R^2 adjusted value of the full model (0.95453).

Table 5.5 shows each of the observed values of Y in both full and reduced model and was compared with the predicted values of Y from each model. The residual value and percent error was calculated to show the correlation between the observed and the predicted values. The low residuals values and percentage error less than 5% show significance of the model used.

Table 5.5
Observed Responses and Predicted Values for Full and Reduced Model MPS

		FULL MODEL			REDUCED MODEL		
Batch No.	**Observed value**	**Predicted value**	**Residual value**	**% Error**	**Predicted value**	**Residual value**	**% Error**
CPNP4	147	147.777	-0.777	0.528	147.611	-0.611	0.415
CPNP5	137	136.777	0.222	0.162	136.777	0.222	0.162
CPNP6	142	141.444	0.555	0.390	141.611	0.388	0.273
CPNP7	137	135.444	1.555	1.095	135.277	1.722	1.256
CPNP8	127	127.444	-0.444	0.349	127.444	-0.444	0.349
CPNP9	134	135.111	-1.111	0.829	135.277	-1.277	0.952
CPNP10	141	141.777	-0.777	0.551	141.611	-0.611	0.433
CPNP11	137	136.777	0.222	0.162	136.777	0.222	0.162
CPNP12	148	147.444	0.555	0.375	147.611	0.388	0.262

The contour plots and the response surface curves give a diagrammatic representation of the values of the response and are shown in Fig. 5.2a and 5.2b for contour plots and the response surface curves respectively drawn at -1 level to 1 level of X1 and X2. The plots were found to be non linear; therefore non linear relationship exists between X1 and X2 variables. It was concluded from the non linear plots of contour and surface response that

the MPS of 153 nm could be obtained with X1 range from 0.2 level (0.22ml) to -0.2 level (0.35ml) and X2 range from 0.2 (3ml) to -0.2 (3ml).

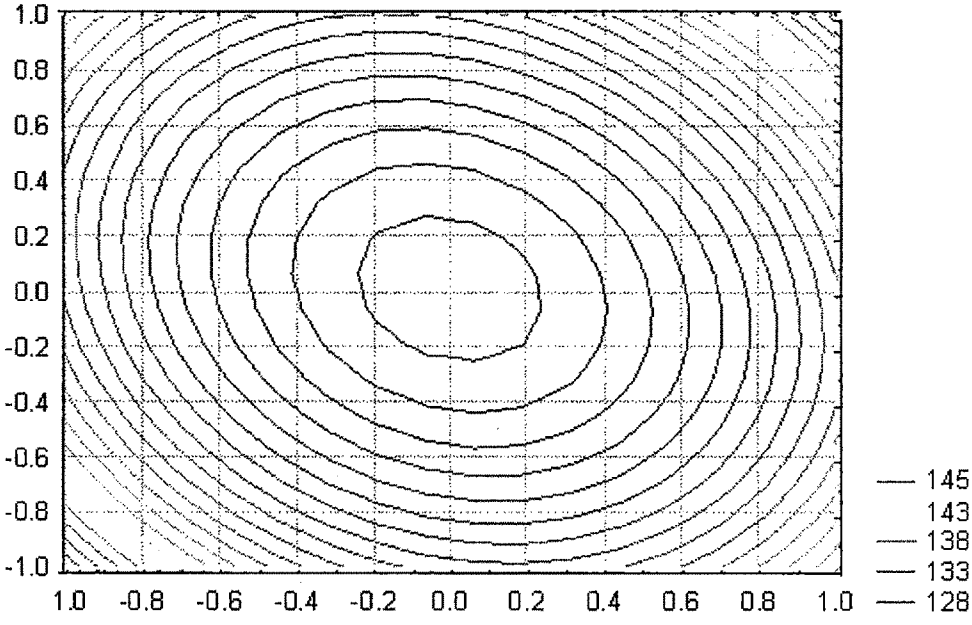

Fig. 5.2a: Contour plot for MPS

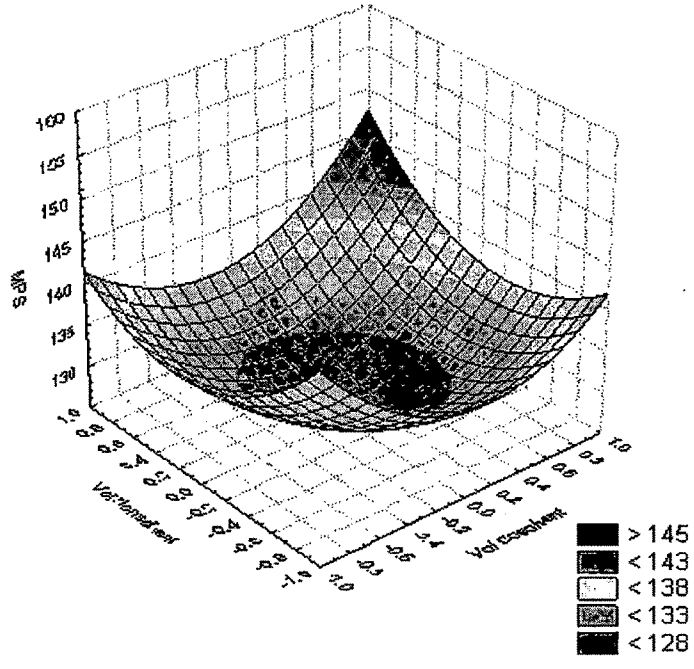

Fig. 5.2b: Surface Response of MPS

5.4.3 Optimization of drug: polymer ratio (for polymer concentration) and stirring time by using Factorial Design for formulation of Cyt-PLGA NP

Nine batches were prepared as per 3^2 factorial design to study the effect of two independent variables, ratio of drug and polymer (X1), stirring time (X2) on the two responses, mean particle size (Y1) and percentage entrapment efficiency (Y2) of the Cyt-PLGA Nanoparticles. Table 5.6 displays the values of Factors, their levels and transformed values and values of the responses, MPS and %EE as per 3^2 factorial design.

Table 5.6
Formulation of Cyt-PLGA NP for optimization of drug:polymer ratio and stirring time. Batches taken as per 3^2factorial design: Factors, their levels and transformed Values and Response: MPS and %EE

	Real value		Transformed values					Response	
Batch No.	Drug: Polymer ratio (mg)	Stirring time (min)	X1	X2	$X1^2$	$X2^2$	X1X2	MPS (nm) ± SD*	% EE ± SD*
CPNP13	1:5	10	-1	-1	1	1	1	142±4.1	15.0±2.3
CPNP14	1:5	20	-1	0	1	0	0	129±3.2	17.8±3.7
CPNP15	**1:5**	**30**	**-1**	**1**	**1**	**1**	**-1**	**125±2.5**	**21.8±2.0**
CPNP16	1:10	10	0	-1	0	1	0	148±2.9	19.6±2.2
CPNP17	1:10	20	0	0	0	0	0	135±3.2	20.0±2.1
CPNP18	1:10	30	0	1	0	1	0	131±4.0	21.6±1.2
CPNP19	1:20	10	1	-1	1	1	-1	151±2.4	20.0±2.1
CPNP20	1:20	20	1	0	1	0	0	139±0.9	21.6±4.2
CPNP21	1:20	30	1	1	1	1	1	134±2.5	22.0±2.1

*Standard Deviation (n=3)

The concentration of drug was kept constant at 5mg/batch, and the concentration of polymer was varied from 25, 50 and 100mg to give drug: polymer ratio of 1:5, 1:10 and 1:20. These three different ratios were tested at three different stirring rates of 10, 20 and 30min and in this way nine batches were prepared as per 3^2 factorial design.

5.4.3.1 Response-Mean Particle Size

The equation for full model for Y1 (MPS) is given by equation 5.3

$$Y1\ (MPS) = 135.222+4.666X1-8.5X2-1.333X1^2+4.166X2^2+0.0X1X2 \qquad (5.3)$$

The mean particle size of NP ranged from 125±2.5 to 151±2.4. The lowest MPS was observed in lowest level of X1 (1:5) and highest level of X2 (30min) in batch CPNP15.

Table 5.7 shows model coefficients estimated by multiple linear regression for MPS. The regression coefficients having P value < 0.05 are highly significant. The terms having coefficients with P value > 0.05 are least contributing in the prediction of mean particle size and hence the factor X1X2 having P value > 0.05 was removed from the full model to give the reduced model equation.

The equation 5.4 explains the reduced model for Y1 (MPS).

$$Y1\ (MPS) = 135.222+4.666X1-8.5X2-1.333X1^2+4.166X2^2 \qquad (5.4)$$

Analysis of Variance (ANOVA) of Full and Reduced Model for MPS is shown in Table 5.8. The F value of Full Model was 813.3, which was more than its tabulated value (F_{tab} = 9.01) suggesting that the full model was significant. F value of the Reduced Model (1355.5) was more than its F_{tab} value (6.39), showing that the model was significant.

Table 5.7
Model Coefficients Estimated By Multiple Linear Regression For MPS

	Full model			Reduced model		
Factor	Coefficient value	Computed t-value	P-value	Coefficient value	Computed t-value	P-value
Intercept	135.222	471.342	2.11E-08	135.222	544.258	6.84E-11
X1	4.666	29.698	8.38E-05	4.666	34.292	4.31E-06
X2	-8.5	-54.093	1.39E-05	-8.5	-62.462	3.94E-07
$X1^2$	-1.333	-4.898	0.0162	-1.333	-5.656	0.0048
$X2^2$	4.1666	15.309	0.0006	4.1666	17.677	6.02E-05
X1X2	0	0	1			

Table 5.8
Analysis of Variance (ANOVA) of Full and Reduced Model for MPS

	Full model		Reduced model	
	Regression	Error	Regression	Error
DF	5	3	4	4
SS	602.444	0.444	602.444	0.444
MS	120.488	0.148	150.611	0.111
F	813.3		1355.5	
Significance f	6.79E-05		1.63E-06	
R^2	0.999263		0.999262	
Adj R^2	0.99803		0.99852	

The R^2 value, which indicates measure of total variability, was more than 0.99 for both the full and reduced models. The R^2 value for the full model was 0.999263, which indicates that the model was highly significant and the model could explain 99.92% of varibility around the mean. The R^2 of the reduced model was also high (0.999262) and could explain 99.92% of variability around its mean, but was lower than the full model, which could be due to less number of factors in the reduced model. In such a case, a higher adjusted R^2 value is expected , if the reduced model is significant (Montegomery, 2004) and in our case there was an increase in the R^2 adjusted value of the reduced model. The R^2 adjusted decreases when non significant terms are added to the equation and removal of non significant terms improves the value of R^2 adjusted. In our case, the value of R^2 adjusted in the reduced model (0.999262809) was greater than the R^2 adjusted value of the full model (0.998034).

Table 5.9
Observed Responses and Predicted Values for Full and Reduced Model MPS

		FULL MODEL			REDUCED MODEL		
Batch No.	**Observed value**	**Predicted value**	**Residual value**	**% Error**	**Predicted value**	**Residual value**	**% Error**
CPNP13	142	141.888	0.111	0.078	141.888	0.111	0.078
CPNP14	129	129.222	-0.222	0.172	129.222	-0.222	0.172
CPNP15	125	124.888	0.111	0.088	124.888	0.111	0.088
CPNP16	148	147.888	0.111	0.075	147.888	0.111	0.075
CPNP17	135	135.222	-0.222	0.164	135.222	-0.222	0.164
CPNP18	131	130.888	0.111	0.084	130.888	0.111	0.084
CPNP19	151	151.222	-0.222	0.147	151.222	-0.222	0.147
CPNP20	139	138.555	0.444	0.319	138.555	0.444	0.319
CPNP21	134	134.222	-0.222	0.165	134.222	-0.222	0.165

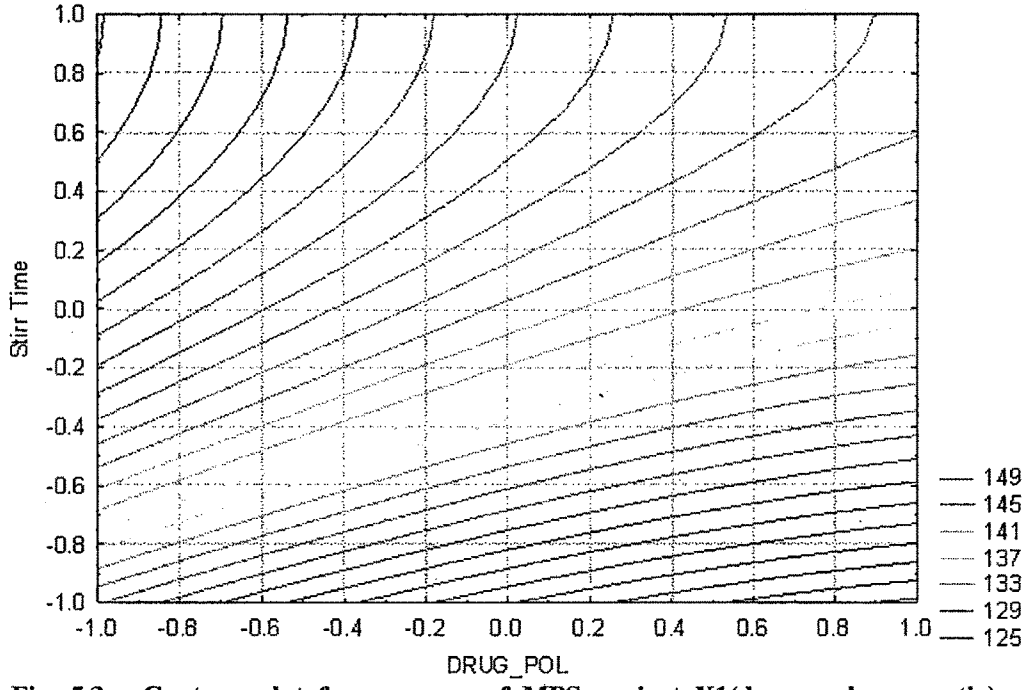

Fig. 5.3a: Contour plot for response of MPS against X1(drug: polymer ratio) and X2 (stirring time) values ranging from -1 to +1.

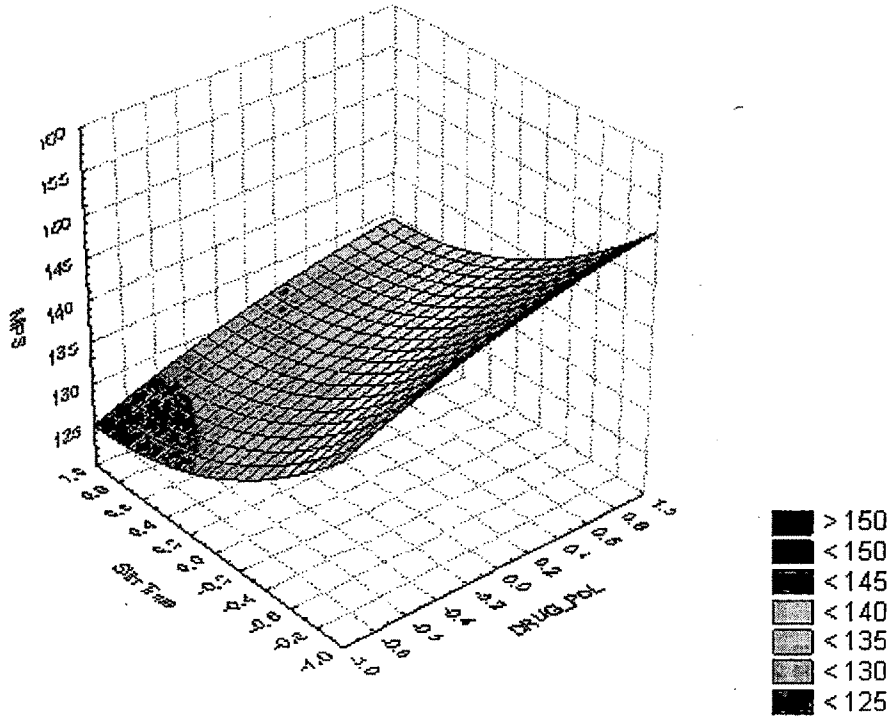

Fig. 5.3b: Surface response plot for MPS against X1(drug: polymer ratio) and X2 (stirring time) values ranging from -1 to +1.

Table 5.9 shows each of the observed values of Y1 (MPS) and was compared with the predicted values of Y from the full and reduced model. The residual value and percent error was calculated to show the correlation between the observed and the predicted values. The low residual values and percentage error less than 5% show significance of the model used.

The contour plots and the response surface curves were drawn at -1 level to 1 level of X1 and are shown in Fig. 5.3a and 5.3b respectively for MPS. The plots were found to be linear; therefore linear relationship exists between X1 and X2 variables. It was concluded from the contour plots and the response surface curves that the MPS of 125 nm could be obtained with X1 range from -0.6 level (1:7) to -1.0 level (1:5) and X2 range from 0.2 (23min) to 1.0 (30min).

5.4.3.2 Response-Entrapment Efficiency

The equation 5.5 is for the full model. The responses in the equation Y2 are the quantitative effect of the formulation components or independent variables X1 and X2.

$$Y2\ (\%EE) = 19.777+1.166X1+1.333X2-0.166X1^2+0.333X2^2-0.5X1X2 \qquad (5.5)$$

The % EE of CYT in PLGA NP varied from 17±2.0% to 22.0±2.1%. Percentage EE of 22.0% was observed at the highest levels of X1 (1:20) and X2 (30min) and % EE of 21.8%, was observed at the lowest level of X1(1:5) and highest level of X2(30min). We chose the batch which had the lower MPS (Batch No.CPN15, %EE of 21.8%).

Table 5.10 shows model coefficients estimated by multiple linear regression for %EE. The regression coefficients having P value < 0.05 are highly significant. The terms having coefficients with P value > 0.05 are least contributing in the prediction of mean particle size and hence the factor $X1^2$ having P value > 0.05 was removed from the full model to give the reduced model equation 5.6.

$$Y2\ (\%EE) = 19.666+1.166X1+1.333X2+0.333X2^2-0.5X1X2 \qquad (5.6)$$

Table 5.10
Model coefficients estimated by multiple linear regression for %EE

	Full model			Reduced model		
Factor	**Coefficient value**	**Computed t-value**	**P-value**	**Coefficient value**	**Computed t-value**	**P-value**
Intercept	19.777	52.113	1.56E-05	19.666	74.629	1.93E-07
X1	1.166	5.612	0.011181	1.166	6.260	0.00332
X2	1.333	6.414	0.007678	1.333	7.155	0.002019
$X1^2$	-0.166	-0.462	0.674941			
$X2^2$	0.333	0.925	0.422826	0.333	1.032	0.360051
X1X2	-0.5	-1.96	0.144294	-0.5	-2.190	0.093599

The results of the regression output and response of full model are presented in Table 4.5 and Analysis of Variance (ANOVA) of full model is presented in Table 5.11. Model F value was assessed by the F statistic, which estimates the percentage of the variability in the outcome explained by the model (Hocking, 1976). Model F value (15.51429) for the full model was more than the tabulated F value ((F_{tab} = 9.01), implying that the model was significant. Similarly, Model F value of the reduced model (24.06667) was more than its corresponding F_{tab} value (6.39) showing that the model was significant.

The R^2value of the full model was 0.962766, explaining 96.27% varibility around its mean. However, the R^2 of the reduced model was lesser than the full model (0.960106383) probably due to less number of factors involved in the reduced model. In such a case, a higher adjusted R^2 value is expected, if the reduced model is significant and in our case there was an increase in the R^2 adjusted value of the reduced model. The value of R^2 adjusted in the reduced model was 0.920212766, which was greater than the R^2 adjusted value of the full model (0.900709).

Table 5.11
Analysis of Variance (ANOVA) of Full and Reduced Model for %EE

	Full model		**Reduced model**	
	Regression	**Error**	**Regression**	**Error**
DF	5	3	4	4
SS	20.111	0.777	20.055	0.8333
MS	4.0222	0.259	5.0138	20.888
F	15.5142		24.066	
Significance F	0.02358		0.0046	
R^2	0.962766		0.96010	
Adj R^2	0.900709		0.92021	

Table 5.12 shows each of the observed values of Y2 which were compared with the predicted values of Y2 from the full and reduced model. The residual value and percent error was calculated to show the correlation between the observed and the predicted values. The low residuals values and percentage error less than 5% show significance of the model used.

Table 5.12
Observed Responses and Predicted Values for Full and Reduced Model %EE

		FULL MODEL			REDUCED MODEL		
Batch No.	**Observed value**	**Predicted value**	**Residual value**	**% Error**	**Predicted value**	**Residual value**	**% Error**
CPNP13	17	16.944	0.055	0.323	17.000	0.000	0.000
CPNP14	18	18.444	-0.444	2.466	18.500	-0.500	2.777
CPNP15	21	20.611	0.388	1.847	20.666	0.333	1.585
CPNP16	19	18.777	0.222	1.168	18.666	0.333	1.752
CPNP17	20	19.777	0.222	1.110	19.666	0.333	1.665
CPNP18	21	21.444	-0.444	2.114	21.333	-0.333	1.585
CPNP19	20	20.277	-0.277	1.385	20.333	-0.333	1.665
CPNP20	21	20.777	0.222	1.057	20.833	0.166	0.790
CPNP21	22	21.944	0.055	0.250	22.000	0.000	0.000

The contour plots and the response surface curves were drawn at -1 level to 1 level of X1 and are shown in Fig. 5.4a and 5.4b respectively for %EE. The plots were was found to be linear with upward and downward segments which indicate linear relationship between X1 and X2 variables. It was concluded from the linear contour and surface response curves that the % EE of 21% could be achieved with X1 range from 1.0to 0.1 level and X2 range from 0.7 to 1.0.

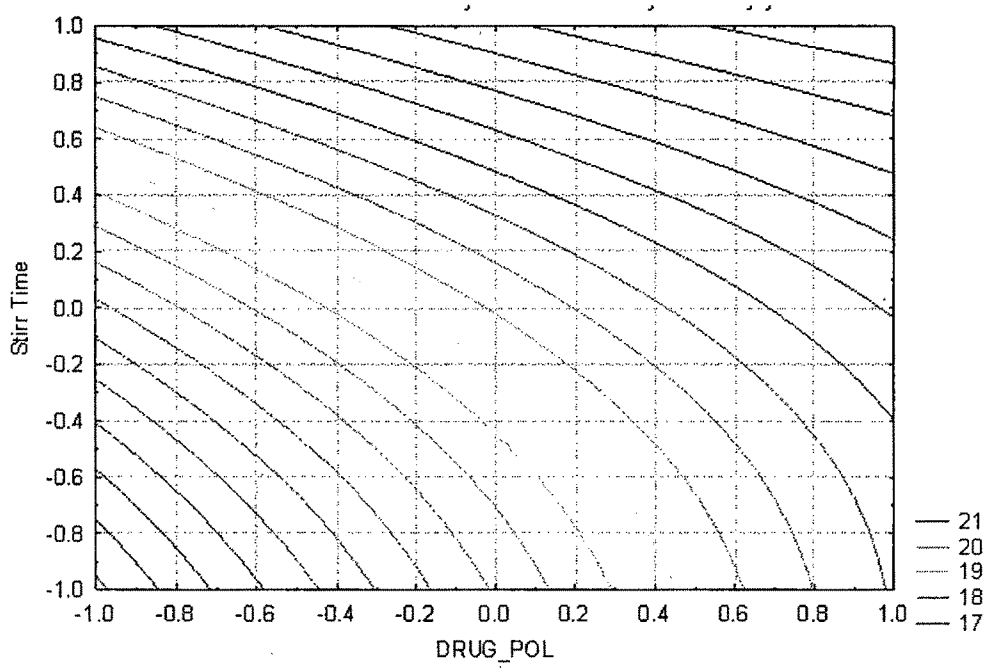

Fig. 5.4a: Contour plot of EE

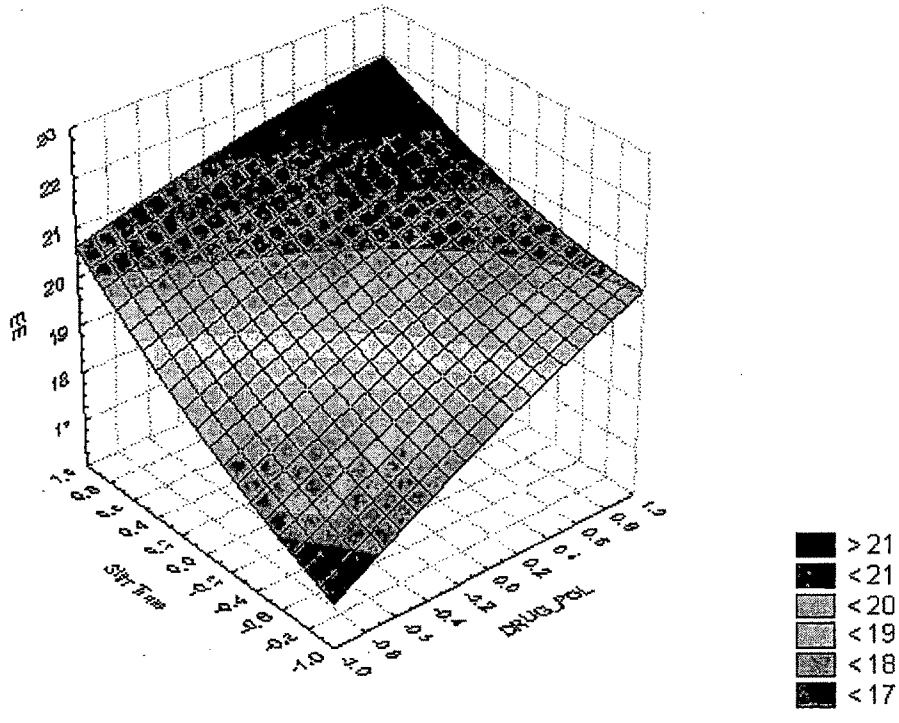

Fig. 5.4b: Surface Response of EE

Fig 5.5 shows Size distribution of batch CPNP15 of Cyt-PLGA NP having MPS of 125.0nm. It was seen that the size distribution curve was bell shaped showing homogenous distribution of particles around the mean.

Fig 5.6 shows zeta potential (-29.7mV) of batch No. CPNP15.

			Diam. (nm)	% Intensity	Width (nm)
Z-Average (d.nm):	125	Peak 1:	120	100.0	35.2
PdI:	0.063	Peak 2:	0.00	0.0	0.00
Intercept:	0.955	Peak 3:	0.00	0.0	0.00

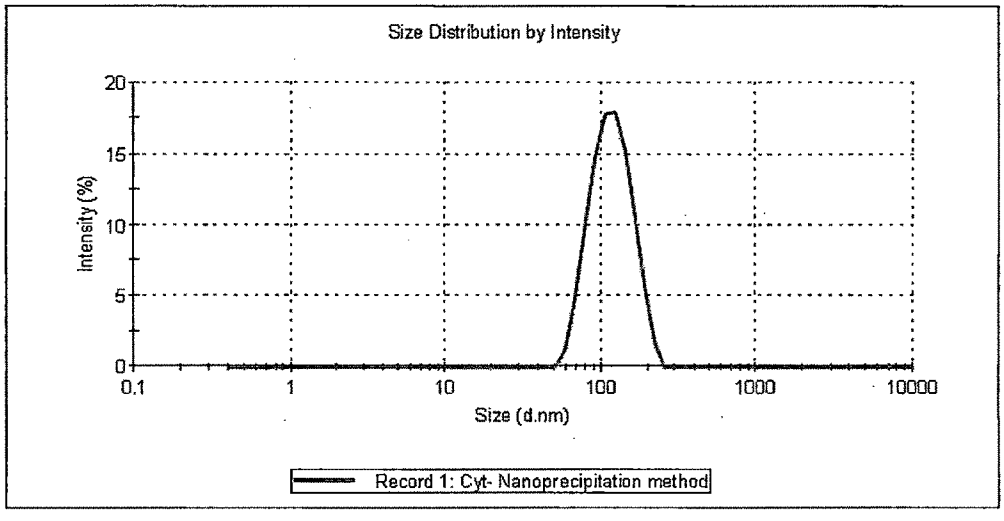

Fig. 5.5: Size distribution graph of Cytarabine loaded PLGA NP batch No. CPNP15

			Mean (mV)	Area (%)	Width (mV)
Zeta Potential (mV):	-29.7	Peak 1:	-29.7	100.0	2.18
Zeta Deviation (mV):	2.18	Peak 2:	0.00	0.0	0.00
Conductivity (mS/cm):	0.0479	Peak 3:	0.00	0.0	0.00

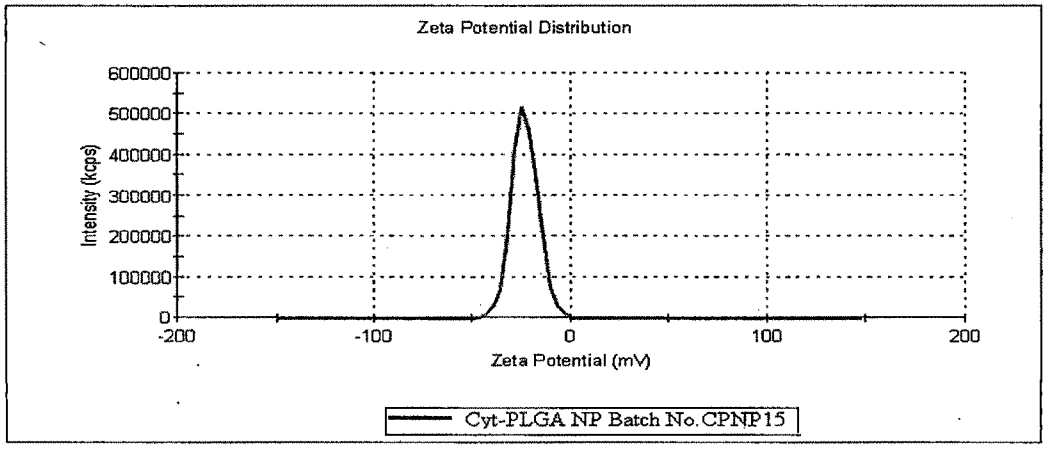

Fig. 5.6: Zeta potential of Cytarabine loaded PLGA NP batch No. CPNP15

5.4.4 Optimization using 3^2 Factorial Design for formulation of Cyt-PLGA-MPEG NP

Nine batches were prepared as per 3^2 factorial design to study the effect of two independent variables, ratio of drug and polymer (X1) and Volume of the non solvent (ml) (X2) on the two responses, mean particle size (Y1) and percentage entrapment efficiency (Y2) of the Cyt-PLGA-MPEG Nanoparticles. Table 5.13 displays the values of Factors, their levels and transformed Values and values of both the responses, %EE and MPS as per 3^2 factorial design.

Table 5.13
Formulation of CYT-PLGA NP batches by 3^2factorial design: Factors, their levels and transformed Values, Response: %EE and MPS

	Real value		Transformed values					Response	
Batch No.	**Drug: Polymer ratio (mg) (X1)**	**Volume of the Non solvent (ml) (X2)**	**X1**	**X2**	**$X1^2$**	**$X2^2$**	**X1X2**	**MPS (nm) ± SD* (Y1)**	**% EE ± SD* (Y2)**
CPM NP1	1:5	2	-1	-1	1	1	1	187± 3.1	29.4±0.3
CPM NP2	1:5	4	-1	0	1	0	0	165± 2.3	32.5±1.2
CPM NP3	1:5	8	-1	1	1	1	-1	152± 6.5	41.1±0.4
CPM NP4	1:10	2	0	-1	0	1	0	192± 5.2	32.6±1.2
CPM NP5	1:10	4	0	0	0	0	0	176± 4.8	35.7±2.2
CPM NP6	1:10	8	0	1	0	1	0	165± 3.2	38.2±3.1
CPM NP7	1:20	2	1	-1	1	1	-1	198± 3.1	36.1±0.8
CPM NP8	1:20	4	1	0	1	0	0	179±2.3	38.4±1.2
CPM NP9	1:20	8	1	1	1	1	1	169±5.7	41.1±0.8

* All the tests were carried out in triplicate

5.4.4.1 Response-Mean Particle Size

The mean particle size of NP ranged from 152±6 to 198±3nm. The lowest MPS was observed in lowest level of X1 (1:5) and highest level of X2 (8ml) in batch CPM NP3.

The equations for full model for Y2 (MPS) is given by equation 5.5

$$Y1\ (MPS) = 175.11-7.0X1-15.16X2-2.66X1^2+3.83X2^2+1.5X1X2 \qquad (5.5)$$

Table 5.14 shows model coefficients estimated by multiple linear regression for MPS. The regression coefficients having P value < 0.05 are highly significant. The terms having coefficients with P value > 0.05 are least contributing in the prediction of mean particle size and hence the factor X1X2 having P value > 0.05 was removed from the full model to generate the reduced model.

Table 5.14
Model coefficients estimated by multiple linear regression for EE.

Factor	Coefficient	Coefficient calculated value	Computed t-value	P-value
Intercept	β_0	175.1111	127.9709	1.05E-06
X1	β_1	7	9.339741	0.002599
X2	β_2	-15.1667	-20.2361	0.000264
$X1^2$	β_{11}	-2.66667	-2.05421	0.132228
$X2^2$	β_{22}	3.833333	2.952927	0.059883
X1X2	β_{12}	1.5	1.634114	0.200745

Analysis of Variance (ANOVA) of full and reduced model for MPS is shown in Table 5.15. The R^2 value for the full model was 0.994179, indicating that the model was able to explain 99.41% variability around its mean in the results. The R^2 value for the reduced model was 0.988997, which was lesser than the full model. This was probably due to the fact that one less factor was involved in the reduced model. In such cases the term R^2

adjusted has to be checked for analyzing the significance of the model. It is called adjusted as the value has been adjusted for the size of the model.. However, in our case, the reduced model had a decreased adjusted R^2 values (0.977994) than that of the full model. Adjusted R^2 values improves because non significant terms are eliminated from full model equation, but in our case it didn't happen. Since the adjusted R^2 values value did not improve the reduced model was not sought and a reduced model was not developed in this case. Full Model F value of 102.4681 was more than the tabulated F value (F_{tab} = 9.01), indicating that the full model was significant.

Table 5.15
Analysis of Variance (ANOVA) of Full and Reduced Model for MPS

	Full model		Reduced model	
	Regression	Error	Regression	Error
DF	5	3	4	4
SS	1726.778	10.11111	1717.778	19.11111
MS	345.3556	3.37037	429.444	4.777778
F	102.4681		89.88372	
Significance F	0.0015		0.000361	
R^2	0.994179		0.988997	
Adj R^2	0.984476		0.977994	

Table 5.16 shows each of the observed values of Y and was compared with the predicted values of Y from the model. The residual value and percent error was calculated to show the correlation between the observed and the predicted values. The low residuals values and percentage error less than 5% show significance of the model used.

Table 5.16
Observed responses and Predicted values for MPS

Batch No.	Observed value	Predicted value	Residual value	% Error
CPM NP1	187	185.9444	1.055556	0.56
CPM NP2	165	165.4444	-0.44444	0.26
CPM NP3	152	152.6111	-0.61111	0.40
CPM NP4	192	194.1111	-2.11111	1.09
CPM NP5	176	175.1111	0.888889	0.50
CPM NP6	165	163.7778	1.222222	0.74
CPM NP7	198	196.9444	1.055556	0.53
CPM NP8	179	179.4444	-0.44444	0.24
CPM NP9	169	169.6111	-0.61111	0.36

The contour plots and the response surface curves were drawn at -1 level to 1 level of X1 and are shown in Fig. 5.7a and 5.7b respectively for MPS. The plots were found to be linear; therefore linear relationship exists between X1 and X2 variables. It was concluded from contour plots and the response surface curves that the MPS of 152 nm could be obtained with X1 range from -1 level (1:5) to -0.7 level (1:6) and X2 range from 0.6 (2.5ml) to 1.0 (8ml).

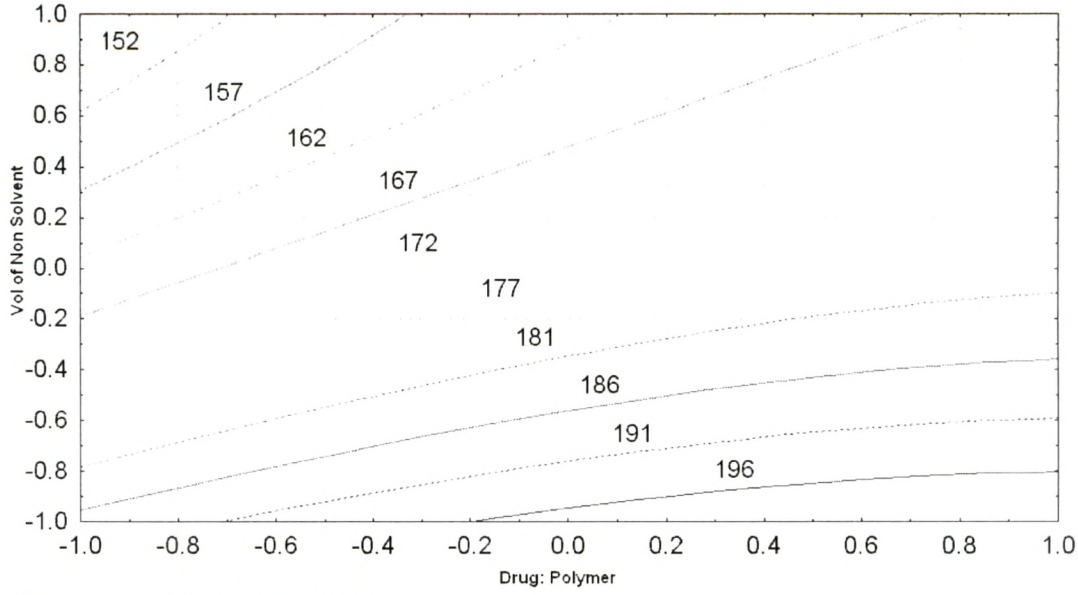

Fig. 5.7a: Contour plot for MPS

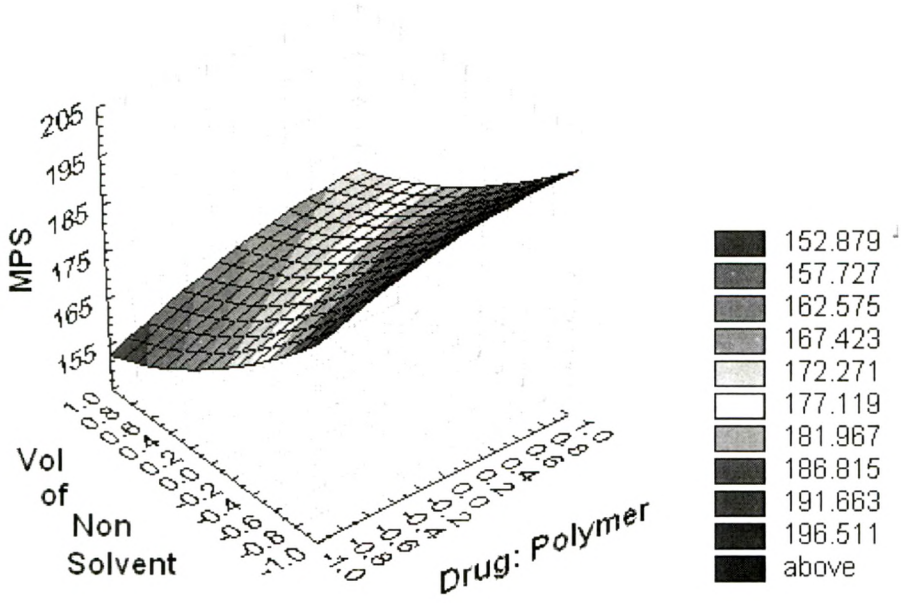

Fig. 5.7b: Surface Response of MPS

5.4.4.2 Response: Entrapment Efficiency

The % EE of CYT in PLGA-MPEG NP varied from 29.4±0.3% to 41.1±0.8%. The highest %EE was observed at two levels of X1 at lowest (1:5)as well as at highest (1:20), but both were obtained at the highest level of X2 (8ml) for batches CPM NP3 and CPM NP9 respectively. The responses in the equation Y2 are the quantitative effect of the formulation components or independent variables X1 and X2. The equation 5.2 is for the full model.

$$Y2\ (\%EE) = 34.91+2.1X1+3.71X2+0.93X1^2+0.88X2^2-2.35X1X2 \qquad (5.6)$$

Table 5.17
Model coefficients estimated by multiple linear regression for EE.

Factor	Coefficient	Coefficient calculated value	Computed t-value	P-value
Intercept	β_0	34.91111	32.8777	6.18E-05
X1	β_1	2.1	3.610742	0.036485
X2	β_2	3.716667	6.39044	0.00776
$X1^2$	β_{11}	0.933333	0.926517	0.422517
$X2^2$	β_{22}	0.883333	0.876882	0.445103
X1X2	β_{12}	-1.675	-2.35151	0.100169

The results of the regression output and response of full model are presented in Table 5.5 and Analysis of Variance (ANOVA) of full model is presented in Table 5.18. Model F value was assessed by the F statistic, which estimates the percentage of the variability in the outcome explained by the model (Hocking RR. 1976). Model F value (12.20642) for this was more than the tabulated F value (F_{tab} = 9.01), implying that the model was significant. The R^2value of the full model was also high (0.953149), indicating that the model was able to explain 95.31% variability in the results. The regression coefficients having P value < 0.05 are highly significant. The terms having coefficients with P value >

0.05 were removed from the model to give the reduced model equation. However, in our case, omitting the terms with P value >0.05 resulted in a reduced model with decreased adjusted R^2 values (Table 5.18). Adjusted R square improves because non significant terms are eliminated from full model equation, but in our case it didn't happen. Since the adjusted r square value did not improve the reduced model was not sought and a reduced model was not developed in this case.

Table 5.18
Analysis of Variance (ANOVA) of Full and Reduced Model for EE

	Full model		Reduced model	
	Regression	Error	Regression	Error
DF	5	3	2	6
SS	123.8669	6.088611	109.3417	20.61389
MS	24.77339	2.029537	54.67083	3.435648
F	12.20642		15.91281	
Significance F	0.032992		0.003991	
R^2	0.953149		0.841377	
Adj R^2	0.875063		0.788503	

The results show that % EE greatly depend on the drug polymer ratio and volume of non solvent. Table 5.19 shows each of the observed values of Y and was compared with the predicted values of Y from the model. The residual value and percent error was calculated to show the correlation between the observed and the predicted values. The low residuals values and percentage error less than 5% show significance of the model used.

Table 5.19
Observed responses and Predicted values for EE

Batch No.	Observed value	Predicted value	Residual value	% Error
CPM NP1	29.4	29.23611	0.163889	0.55
CPM NP2	32.5	33.74444	-1.24444	3.81
CPM NP3	41.1	40.01944	1.080556	2.62
CPM NP4	32.6	32.07778	0.522222	1.60
CPM NP5	35.7	34.91111	0.788889	2.20
CPM NP6	38.2	39.51111	-1.31111	3.42
CPM NP7	36.1	36.78611	-0.68611	1.88
CPM NP8	38.4	37.94444	0.455556	1.18
CPM NP9	41.1	40.86944	0.230556	0.55

The contour plots and the response surface curves were drawn at -1 level to 1 level of X1 and are shown in Fig. 5.8a and Fig 5.8b. The plots of EE were found to be linear with upward and downward segments which indicate linear relationship between X1 and X2 variables. It was concluded from the linear contour plots and the response surface curves that the % EE of 41% could be achieved with X1 in two different levels of 0.2 to 1.0 as well as -0.2 to -1.0 and X2 range at 0.6 level to 1.0 level.

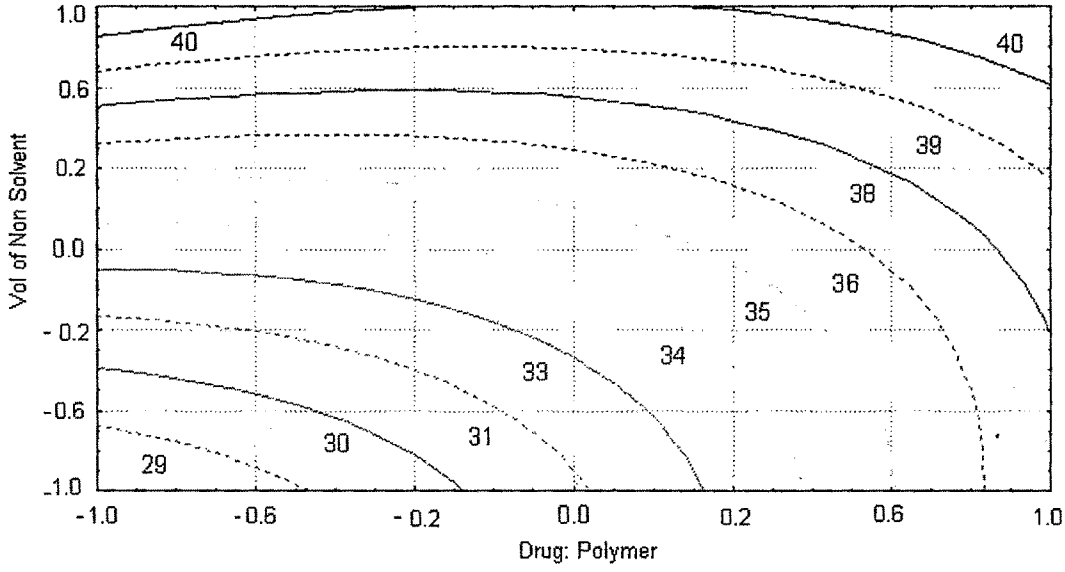

Fig. 5.8a: Contour plot of EE

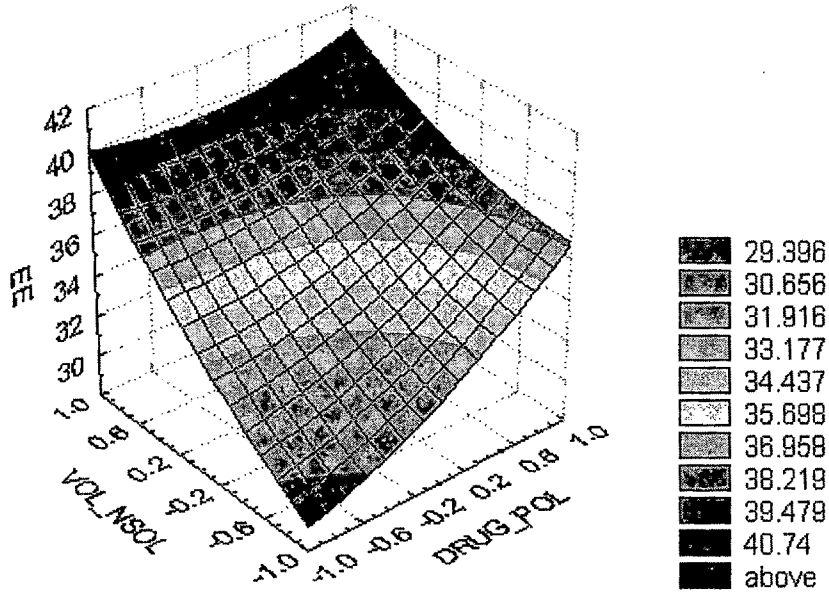

Fig. 5.8b: Surface Response of EE

5.4.5 Lyophilization and optimization of cryoprotectant

Lyophilization is the process in which freeze-drying is done to remove solvent from the formulation and therefore improve its stability upon storage. The process of freeze drying is stressful and hence a cryoprotectant is added in the process, which also helps in redispersibility of the freeze-dried nanoparticle in a suitable solvent (Chacon et al. 1999). One of the main challenges during the freeze drying process is preserving or rather increasing the redispersibility of the nanoparticles upon reconstitution with distilled water or buffer saline. Redispersants are generally added to the nanoparticles prior to the drying step. Commonly used cryoprotectants such as sugars also act as redispersants. Cryoprotectants such as sorbitol, mannitol, glucose, trehalose can be used to increase the physical stability of nanoparticles during freeze-drying (De Chasteigner et al. 1996); Molpeceres et al. 1997).

In the present study we have used sucrose in five different concentrations of 10, 20, 50, 75 and 100%w/w to act as both a cryoprotectant and a redispersant.

Freeze-drying has an effect of increasing particle size after lyophilization, probably due to aggregation of nanoparticles during this process; therefore we checked the redispersibility of the particles after lyophilization. If the aggregated particles do not separate during redispersion, then larger particle sizes will be observed which are not desired.

Table 5.20 indicates the different concentrations of sucrose used and is effect on particle size after lyophilization. Optimization of the cryoprotectant was based on its ability to give minimum increase in size and dispersibility. An increase in size of the NPs was seen following freeze-drying with the use of sucrose as cryoprotectant. All the formulations above 50% w/w sucrose had good dispersibilty and it was seen that use of sucrose in a 50%w/w concentration showed minimum increase in particle size of the Cyt-PLGA NP. 20% w/w sucrose was optimum for Cyt-PLGA-MPEG NP as after lyophilization it had minimum increase in MPS. Use of higher concentrations of cryoprotectants made the NP dispersible but an increase in MPS was also observed. So higher concentrations of more than 20% w/w for Cyt-PLGA-MPEG NP and 50% w/w for Cyt-PLGA NP were not selected. .

Table 5.20
Optimization of Sucrose as cryoprotectant and its effect on mean particle size and redispersibility

% w/w Sucrose	Cyt-PLGA NP				Cyt-PLGA-mPEG NP			
	Mean particle size		Redispersibility		Mean particle size		Redispersibility	
	BL	AL	MS	SO	BL	AL	MS	SO
0	125	212	ND	ND	152	205	ND	ND
10	125	149	ND	ND	152	172	ND	ND
20	125	135	ND	D	152	155	D	D
50	125	129	D	D	152	165	D	D
75	125	147	D	D	152	168	D	D
100	125	152	D	D	152	172	D	D

BL- Before Lyophilization, AL- After Lyophilization, MS- Manual shaking, SO-Sonication, D-dispersible, ND- non dispersible.

It was concluded that 20% w/w sucrose in Cyt-PLGA-MPEG NP and 50% w/w of sucrose in Cyt-PLGA NP can be added as cryoprotectant during lyophilization for freeze dried NPs having good dispersibility with minimum increase in their mean particle sizes.

5.4.6 SEM studies

The electron micrograph showed spherical and discrete particles in the nanometer size range (Fig. 5.9).

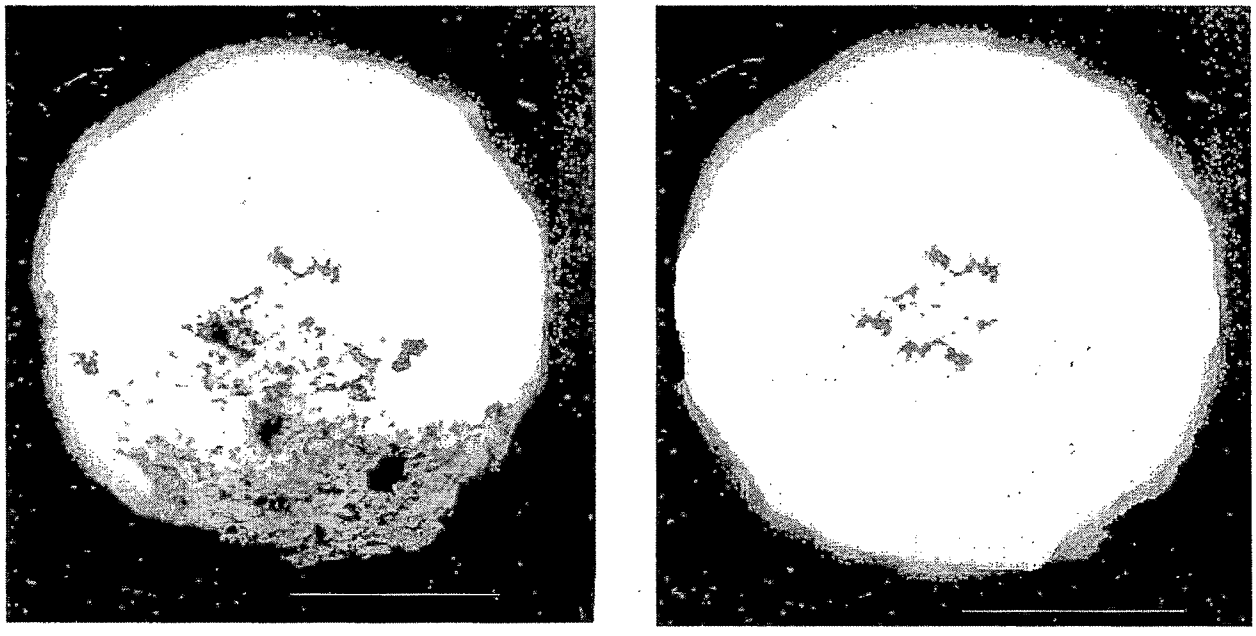

A. Cyt-PLGA NP

B. Cyt-PLGA-MPEG NP

Fig. 5.9: SEM of Cyt-PLGA NP and Cyt-MPEG NP. The bar line indicates 50nm

5.4.7 X-ray powder diffraction studies

X-ray powder diffraction studies (Fig. 5.10) showed that crystal peaks of Drug (CYT) were visible in plain drug but were not seen in Nanoparticles. Hence it could be concluded that in the prepared Cyt-PLGA NP and Cyt-PLGA-MPEG NP, the drug was present in the amorphous phase and may have been homogeneously dispersed in the polymer matrix.

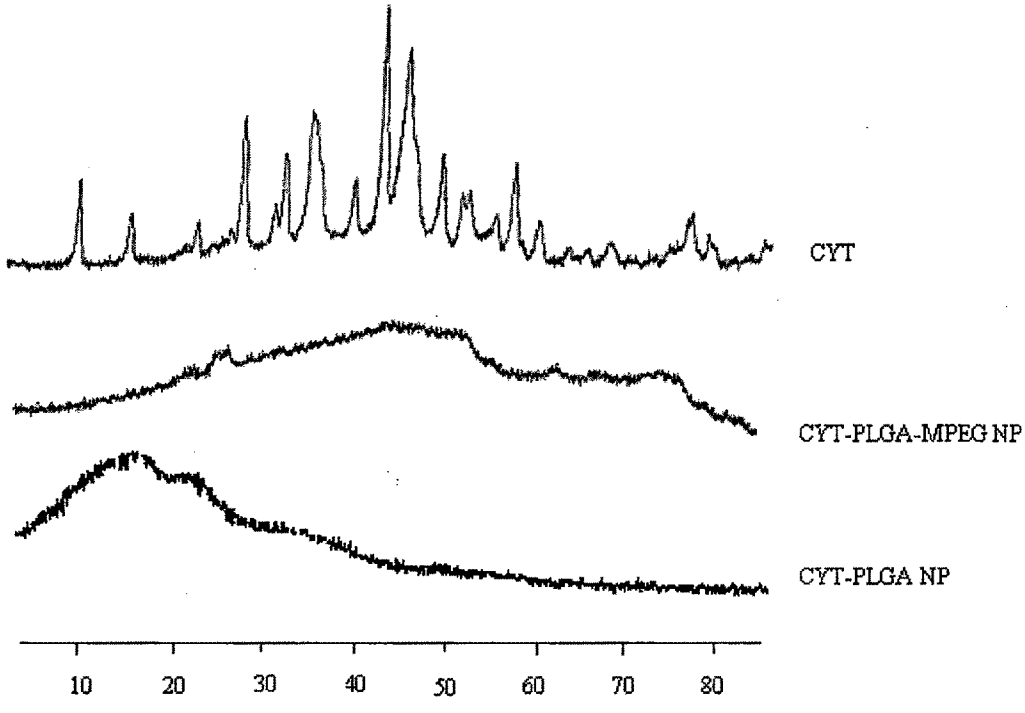

Fig. 5.10: XRD of cytarabine, Cyt-PLGA NP and Cyt-PLGA-MPEG NP

5.4.8 DSC studies

Differential Scanning Calorimetry (DSC) gives information regarding the physical properties like crystalline or amorphous nature of the samples (Sophie-Dorothée et al., 1999). The DSC thermograms (Fig. 5.11) of cytarabine, PLGA and Cyt-PLGA NP depicted characteristic endothermic peaks. Onset of cytarabine was seen at 211.13 °C, endset at 218.20 °C and the peak was at 213.94 °C. PLGA had onset at 51.60 °C, endset was seen at 56.17 °C and peak at 54.11 °C. Cyt-PLGA NP had onset at 54.81 °C, endset 62.04 °C and peak at 58.02 °C. These endothermic curves showed that the drug peak was absent in nanoparticle formulation, indicating drug was dispersed as an amorphous state in the nanoparticle (Mandal et al., 2002). Hence it could be concluded that in the prepared PLGA NP, the drug was present in the amorphous phase and may have been homogeneously dispersed in the PLGA matrix.

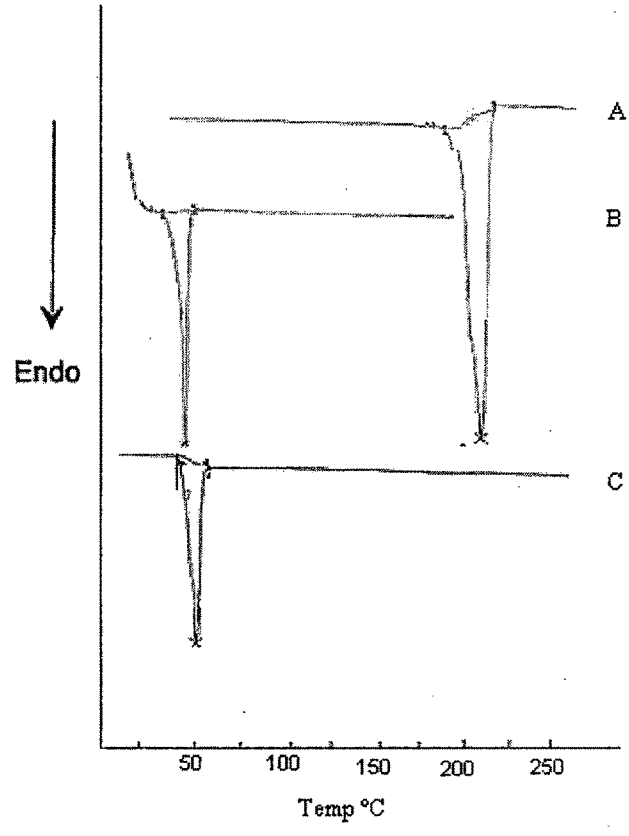

Fig. 5.11: DSC thermogram of (A) cytarabine, (B) PLGA and (C) Cyt-PLGA NP

5.4. 9 In vitro drug release

In vitro drug release from the pure drug was complete within 2 hours, but was sustained up to 2 days from PLGA-mPEG nanoparticles and 1 day from PLGA nanoparticles. The release profile is shown in Table 5.21 and Fig. 5.12.

Cytarabine loaded PLGA NP (CPN) released 34% in 1h and 51% in 2h. The release from Cyt-PLGA NP was sustained till 24h.CYT loaded PLGA-mPEG Nanoparticles (CPM NP) released 24% in 1h and 29% in 2h. PLGA-MPEG NPs were able to sustain the release up to 48h.

The sustained release of the drug may be attributed to the PLGA's property to sustain the release of the entrapped drug in nanoparticles (Lamprecht et al., 2000). Comparison of the R^2 value of zero order and first order (Table 5.21) showed that R^2 value of first order was higher in both cases than the zero order, indicating that the release followed first ordered kinetics in both the cases (Fig. 5.13). The high R^2 values (> 0.99) of first order showed that the release was time dependent. Data fitted to Higuchi model (Fig 5.14) showed that CPM NP had high R^2 value (> 0.95) indicating that drug release from CPM NP follows Higuchi diffusion kinetics.

The release data were fitted to Korsmeyer and Peppas equation (Korsmeyer et al., 1983; Peppas, 1985) and Diffusion exponent (n value) was obtained from the slope (Fig. 5.15) and was found to be 0.3754 for CPNP and 0.411 for CPM NP (Table 5.22). In both the cases, the n value was less than 0.43 indicating a Fickian release mechanism from both the NP.

It was concluded from the drug release studies that PLGA NP could sustain the release of CYT upto 24h and the release mechanism was Fickian diffusion and it followed first order kinetics. PLGA-mPEG NP on the other hand could extend the release upto 48h and followed first order kinetics. The Higuchi model was obeyed in this case and the drug release mechanism was Fickian diffusion.

Table 5.21

In Vitro Drug Release Profile of CYT and CYT loaded NP

Time (h)	% Drug Released		
	Cyt	CPM NP	CPNP
0.5	38.5±3.1	11±1.5	21±3.5
1	82.4±4.2	24±2.0	35±2.2
2	98.5±2.1	29±3.5	51±2.4
4		40±2.2	63±3.3
6		54±2.5	78±3.9
12		70±3.0	88±4.2
24		88±4.1	99.7±1.2
36		96±4.5	
48		98.9±1.5	

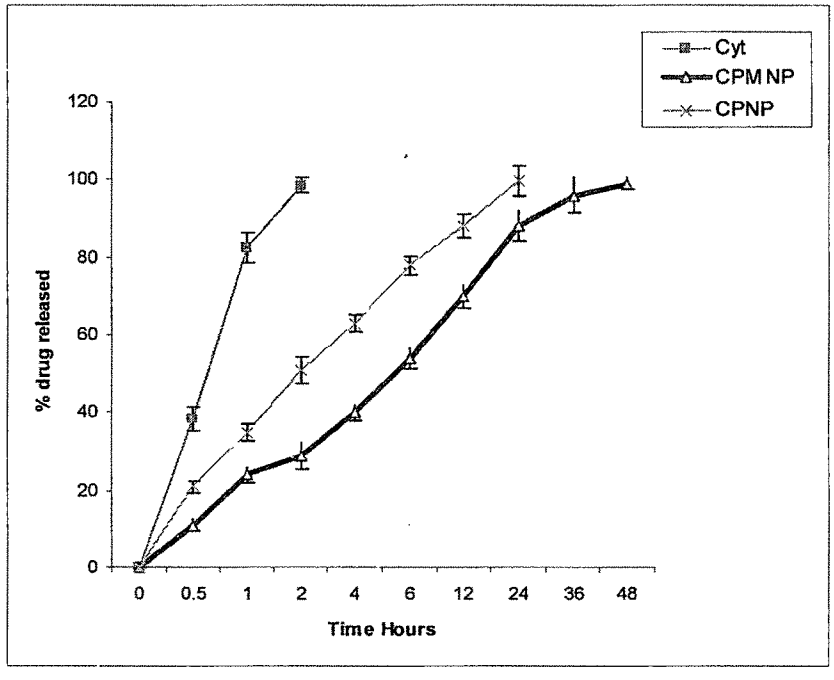

Fig. 5.12: In Vitro Drug Release Profile of Cytarabine pure drug, Cytarabine loaded PLGA-mPEG NP (CPM NP)and Cytarabine loaded PLGA Nanoparticles (CPNP)

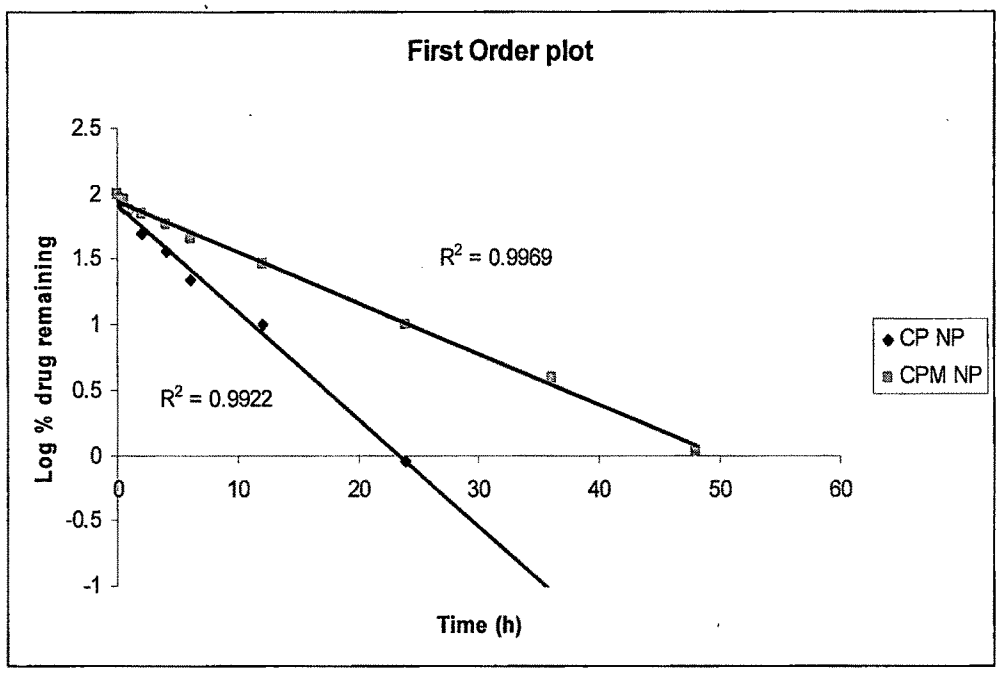

Fig 5.13: First Order Plot

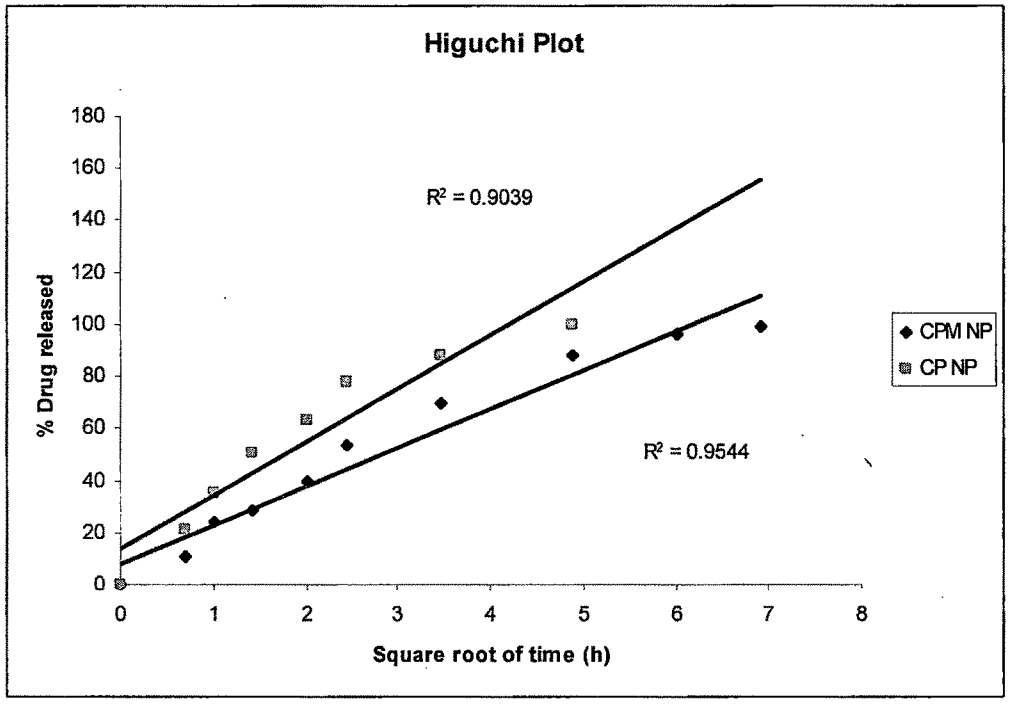

Fig 5.14: Drug Release Fitted to Higuchi Model

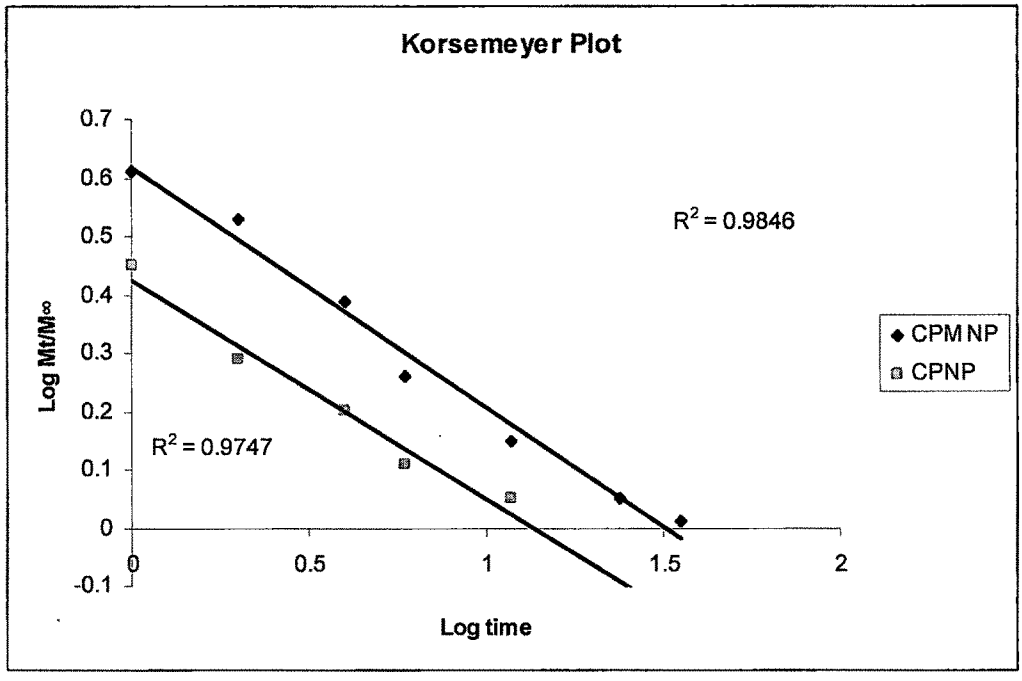

Fig 5.15: Korsmeyer-Peppas model for CPM NP and CPNP, Log (Mt/M∞) is plotted against Log time t

Table 5.22
Drug release Kinetics

	CP NP			CPM NP		
	Linearity Equation	**R^2 value**	**slope**	**Linearity Equation**	**R^2 value**	**slope**
Zero order	y = 3.4406x + 33.174	0.6738	3.4406	y = 1.8906x +25.85	0.8001	1.8906
First order	y = -0.0821x + 1.9202	0.9922	-0.0821	y = -0.039x + 1.942	0.9969	-0.039
Higuchi	y = 20.548x + 13.623	0.9039	20.548	y = 14.855x + 8.2792	0.9544	14.855
Korsemeyer	y = 0.3754x + 0.4257	0.9747	0.3754 (n value)*	y = 0.411x + 0.6187	0.9846	0.411 (n value)*

* n value is the diffusion coefficient obtained from slope of Korsemeyer plot

5.4.10 Stability studies

Stability studies of polymeric nanoparticles were carried out to evaluate the change in mean particle size and drug content over a period of three months storage at 2-8, 25 and 40°C.

Storage at 2-8°C

For cytarabine loaded PLGA-mPEG NP (CPM NP3) as well as cytarabine loaded PLGA NP (CPNP15) there was no significant change ($P>0.05$) in the mean particle size and drug content at 2-8°C for 1 and 2M (Fig 5.16 and 5.17). There was significant change ($P>0.05$) in the mean particle size and drug content of both CPM NP3 and CPNP15 at 3M. The MPS of CPM NP3 increased from initial 155nm to 162nm in 3M and the MPS of CPNP15 increased from initial 129nm to 142 nm in 3M. The drug content for CPM NP3 decreased to 96% in the 3M and the drug content of CPNP15 decreased to 96% in the 3M.

Storage at 25°C

For cytarabine loaded PLGA-mPEG NP (CPM NP3) as well as cytarabine loaded PLGA NP (CPNP15) there was no significant change ($P>0.05$) in the mean particle size and in drug content at 25°C for 1M (Fig 5.16 and 5.17). But there was a significant change in the mean particle size and % EE of both CPM NP3 and CPNP15 at 25°C for 2 and 3M. The size of the particles increased significantly in the 2 and 3M. The MPS of CPNP15 increased from initial 129nm to 138 and 148nm in 2 and 3M respectively. The MPS of CPM NP3 increased from initial 155nm to 164 and 171 nm in 2 and 3M respectively. The drug content for CPNP15 decreased to 92 and 81% in the 2 and 3M respectively. The drug content of CPM NP3 decreased to 92 and 85% in the 2 and 3M respectively.

Storage at 40°C

Cytarabine loaded PLGA-mPEG NP (CPM NP3) as well as cytarabine loaded PLGA NP (CPNP15) were not stable at 40°C as there was significant change (P>0.05) in both the mean particle size and in the drug content (Fig 5.16 and 5.17). The MPS of CPM NP3 increased from initial 155nm to 163, 178 and 180nm in the 1, 2 and 3M respectively. The MPS of CPNP15 increased from initial 129nm to 141, 163 and 172 nm in 1, 2 and 3M respectively. The drug content of CPM NP3 decreased to 90, 82 and 71% in the 1, 2 and 3M respectively. The drug content of CPNP15 decreased to 89, 83 and 68% in the 1, 2 and 3M respectively.

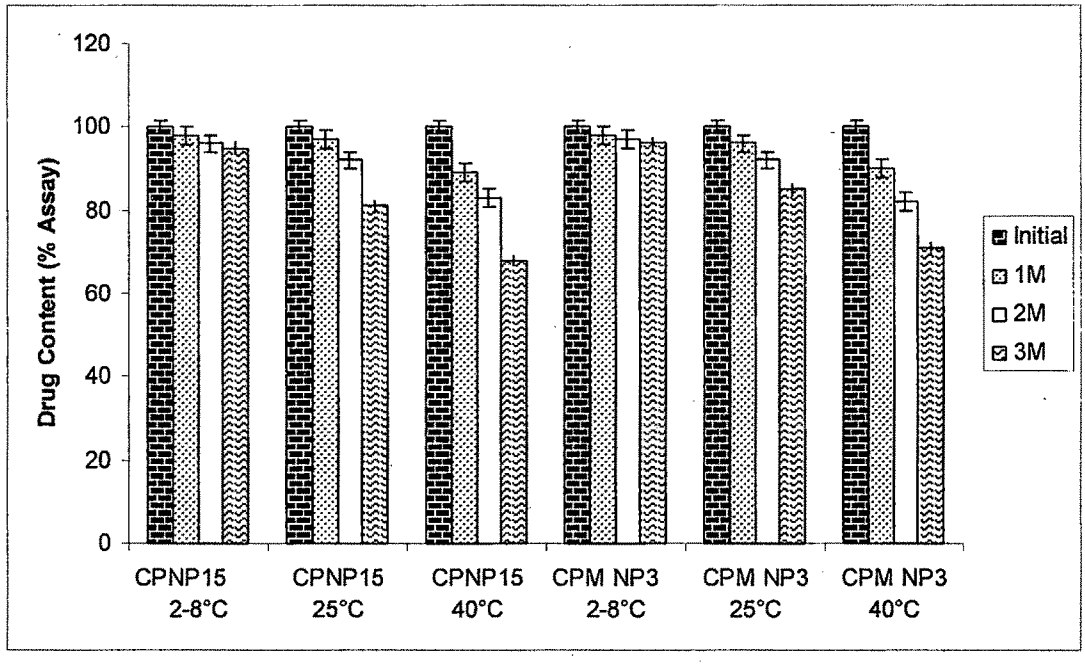

Fig. 5.16: Effect of storage at 2-8°C, 25°C and 40°C on drug content of Lyophilized Cytarabine loaded PLGA NP (CPNP15) and Cytarabine loaded PLGA-mPEG NP (CPM NP3). The values are mean of three batches with ± S.D

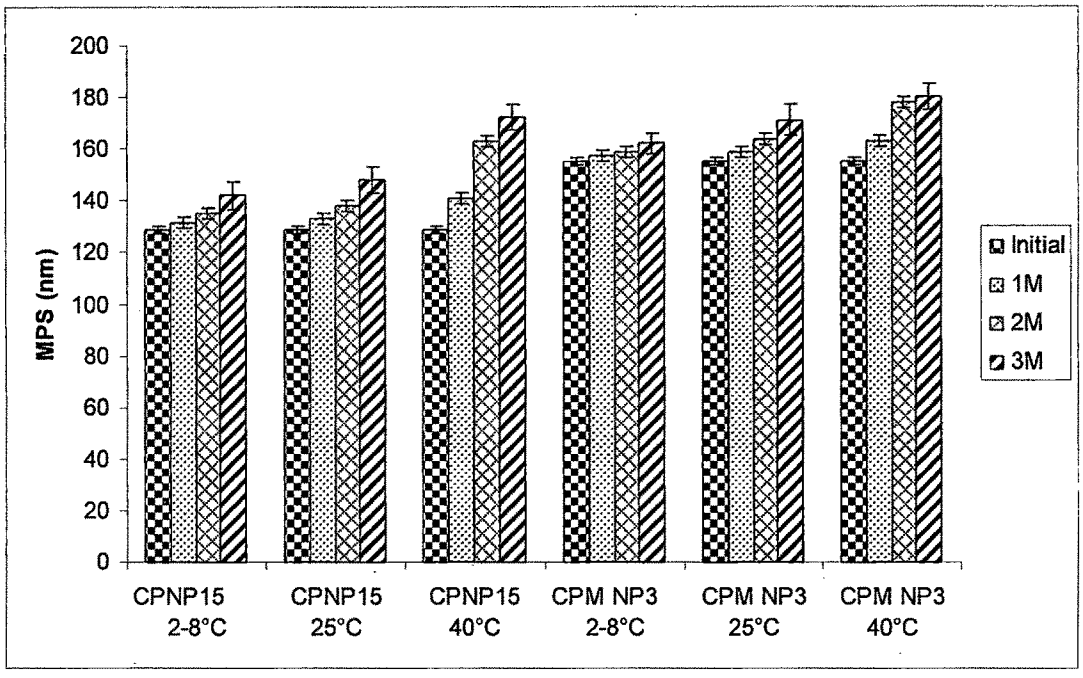

Fig. 5.17: Effect of storage at 2-8°C, 25°C and 40°C on Mean Particle Size (MPS) of Lyophilized Cytarabine loaded PLGA NP (CPNP15) and Cytarabine loaded PLGA-mPEG NP (CPM NP3). The values are mean of three batches with ± S.D

Conclusion

It as observed from the stability studies that cytarabine loaded PLGA-mPEG NP (CPM NP3) and cytarabine loaded PLGA NP (CPNP15) were stable at 2-8°C for 2M and at 25°C for 1M as there was no significant change in the mean particle size and in the drug content. Nanoparticles are not stable at higher temperatures (> 25°C) due to aggregation of particles and degradation of the polymer (Dunne et al., 2000).

It was concluded that the developed PLGA NPs should be stored in the freeze dried state at 2-8°C where they would remain stable in terms of both MPS and drug content.

REFERENCES

Chacon M, Molpeceres J, Berges L, Guzman M, Aberturas MR (1999). Stability and freeze-drying of cyclosporine loaded poly(D,L lactide-glycolide) carriers. *European Journal of Pharmaceutical Sciences 8*, 99–107.

De Chasteigner S, Cave´ G, Fessi H, Devissaguet J-P, Puisieux F (1996). Freeze-drying of itraconazoleloaded nanosphere suspensions: A feasibility study. *Drug Development Research 38*, 116–124.

Freitas and Muller RH (1998). Spray-drying of solid lipid nanoparticles (SLN^{TM}), *European Journal of Pharmaceutics and Biopharmaceutics 46*, 145–151.

Hocking RR (1976). Analysis and selection of variables in linear regression. *Biometrics 32*, 1-49.

Kesisoglou F, Panmai S, Wu Y (2007). Nanosizing-Oral formulation development and biopharmaceutical evaluation. *Advanced Drug Delivery Reviews 59*, 631–644.

Korsmeyer RW, Gurny R, Doelker E, Buri P, Peppas NA (1983). Mechanisms of solute release from porous hydrophilic polymers. *International Journal of Pharmaceutics 15*, 25-35.

Lamprecht A, Ubrich N, Hombreiro Pérez M, Lehr CM, Hoffman M, Maincent P (2000). Influences of process parameters on nanoparticle preparation performed by a double emulsion pressure homogenization technique. *International Journal of Pharmaceutics 196*, 177-182.

Levy MY and Benita S (1990). Drug release from submicronized o/w emulsion: a new in vitro kinetic evaluation model. *International Journal of Pharmaceutics 66*, 29–37.

Mandal TK, Bostanian LA, Graves RA, Chapman SR, Womack I (2002). Development of Biodegradable Microcapsules as Carrier for Oral Controlled Delivery of Amifostine. *Drug Development and Industrial Pharmacy 28(3)*, 339– 344.

Montegomery DC (2004). Design and analysis of experiments, John Wiley and sons. 392-426.

Peltonen L, Aitta J, Hyvönen S, Karjalainen M and Hirvonen J (2004). Improved Entrapment Efficiency of Hydrophilic Drug Substance During Nanoprecipitation of Poly(l)lactide Nanoparticles. *AAPS PharmSciTech 5 (1)*, Article 16.

Peppas NA (1985). Analysis of Fickian and non-Fickian drug release from polymers. *Pharm. Acta. Helv. 60*, 110-11.

Siepmann and Peppas NA (2001) Modeling of drug release from delivery systems based on hydroxypropyl methylcellulose. *Advanced Drug Delivery Reviews 48*, 139–157.